Acta Technica *62* No. 3A/2017, 321–334

Modeling and kinematics simulation of freestyle skiing robot

Xiaohua Wu[1,3], Jian Yi[2]

Abstract. Freestyle skiing robot model and gait planning are used for the robot model moving in the snow. First, data of human body is collected by 3-D laser scanning technique. Sports biomechanics and computer simulation methods are used to structural design and analyze freestyle skiing robot. Then, 3-D modeling software Pro/E is used to build entity model then gait planning based on bionics is studied. Finally, virtual prototype technology is used to modeling the robot at the slipping stage to verify the feasibility of gait planning. Results show that slipping stage can be dynamically simulated by the freestyle skiing robot. Displacement and velocity change of joints of theoretical movement are very close to that of simulation movement. Moreover, theoretical angular acceleration curve is relatively close to simulation results. In conclusion, gait planning of bionics is suitable for motion planning of freestyle skiing robot and robots' all movements at slipping stage can be achieved.

Key words. Freestyle skiing robot, ADAMS, Pro/E, gait planning, kinematics.

1. Introduction

Robotics is widely used in modern production, national economy and people's livelihood with the development of modern science and technology. Among all kinds of robot, system structure of humanoid robot is the most complex one and its integration level is high, which represents the cutting-edge technology of robot and is essential for study robot [1].

2. Literature review

Nowadays, humanoid robot has entered an essential stage where intended functions can be realized. Humanoid robot is on the cutting edge of robot research,

[1]Jilin Sport University, Jilin, 130022, China
[2]College of Humanities & Information, Changchun University of Technology, Changchun, 130122, China
[3]Corresponding author; E-mail: xiaohuawuxh@126.com

which is important for research on humanoid robot [2]. Problems occurred during research and development of humanoid robot product of long development cycle and expensive cost cannot be solved by traditional design flow of physical prototype. Virtual prototype technology is used to assist study, such as kinematic modeling and simulation, dynamics simulation and analysis and optimization design of structure of humanoid robot [3]. Virtual prototype technology advances the development of humanoid robot greatly. With their development and combination, more and more kinds of humanoid robots are produced, for example soccer robot, basketball robot and running robot.

Ontological mechanical structure of freestyle skiing robot is designed based on characteristics of physical structure of freestyle skiing athlete and motion mechanism analysis of human skeleton and muscle. Design thought and implementation method for lower limbs, trunk, upper limbs and head are put forwarded according to different functions of joints and body parts [4]. Bionic gait planning method is adopted for freestyle skiing robot on the basis of existing experimental data of freestyle skiing robot and feature of mechanical structure. Cubic spine interpolation algorithm is used to planning joints track of hip, knee, shoulder and elbow. Virtual prototype model of freestyle skiing robot is built in ADAMS then track planning parameters of joints are used to generate STEP function which is added to corresponding joints of freestyle skiing robot in virtual prototype. Thus, simulation experiment for freestyle robot is conducted and the simulation results show that bionic gait planning is feasible and all movements of robot at slipping stage can be achieved.

3. Methods

3.1. Structural design and analysis of freestyle skiing robot

3.1.1. Body frame and structure design. Below aspects should be taken into consideration when designing body frame of freestyle skiing robot- First, size (height and weight) of body frame should be identified according to human body proportion. Second, main control computer, data acquisition card (DAQ Card), motor driver, and power management module were installed and carried on body frame, for which rational distribution and load bearing strength and stiffness of body frame should be considered. Third, heat dissipation of motor drive and main control computer should be taken into account when designing body frame [5].

3.1.2. Joint structure design and analysis for lower limbs. Limbs structure of freestyle skiing robot was symmetrical, which meant structure of left and right legs was the same. Thus, structural design of left leg was taken as an example. There were six rotary joints in the left leg of the robot.

1) Structural design and analysis of hip joint

For inverse kinematics solution of leg, axes of hip joints in three directions should meet in one point, thus there was closed-form solution. It meant that DOF (degree of freedom) of joint rotation, roll and pitching should meet in one point. Mechanical

structural of DOF of hip joint pitching and roll was made up of servo motor, synchronous belt and harmonic reducer. Servo motor and reducer were near joint and power was output to joint through synchronous belt. There was small moment of inertia while large driving torque because synchronous belt was directly connected to joint which is not suitable to precision positioning.

2) Structural design and analysis of knee joint

Drive capability of knee joint was important for robot movement because it supported upper body and carried outfast start and stop functions. Dual motor drive and V-belt pulley were used to knee joint, with which there were two advantages. First, due to dual motor drive, there was superposition of output torque of electric machine. Thus, capability of joint to output torque was improved and heat caused by long-working time was avoided. Second, the small-adjustment eccentric tensioning wheel was adopted by driving mechanism of knee joint. Thus, distances between input axis of knee joints can be adjusted by changing installation angle of the small-adjustment eccentric tensioning wheel. Counting-rate-difference feedback signal of dual motor can be acquired by two encoders in real time, which was convenient for master-slave control of dual-motor, joint angle information acquisition, mechanical transmission error correction and control accuracy improvement.

3) Structural design and analysis of ankle joint

According to bionics principle, ankle joint was of two degrees of freedom - pitching and roll. Besides, those two axes were met in one point, which was similar to structure of hip joint. Also, modular design method was used to design degree of freedom of pitching and roll of ankle joint and it was made up of servo motor, harmonic reducer and synchronous belt. There was a criss-cross construction at its pitching and roll joints, because of which there were a compact structure of ankle joint and a downsized ankle joint. Potentiometers were put on degree of freedoms of pitching and roll of criss-cross construction joint to detect practical output angle of joint.

3.1.3. Structural design and analysis of the upper arm joint. This structural design was similar to that of hip joint. According to document literature, as long as axis of shoulder joint in three directions was met in one point, there was closed-form solution of the upper arm when conducting inverse kinematics solution. It meant that when designing, DOF (degree of freedom) of rotation, roll and pitching of shoulder joint should met in one point.

3.1.4. Design and analysis of waist joint and neck joint. Two structural designs have to be considered.

1) Structural design and analysis of waist joint

In this design method, there were two degree of freedoms for waist – pitching and roll. Electric machine 1 was used to control pitching degree of freedom of waist joint by transmitting power to harmonic reducer. Then, waist support frame was controlled by reducer to support its pitching movement. Besides, the other end of

waist support frame was connected to bearing. Electrical machine 2 was used to control the waist rotation by transmitting power to harmonic reducer. Then, waist rotation support frame was controlled by reducer to support its rotation movement through sleeve.

2) Structural design and analysis of head joint

There were two degree of freedom for head – pitching and rotation. Electrical machine 1 was used to control pitching degree of freedom by transmitting power to harmonic reducer. Then, head support frame was controlled by reducer to support head pitching movement. Besides, the other end of head pitching support frame was connected to bearing. Electrical machine 2 was used to control rotation joint of head by transmitting power to harmonic reducer. Support frame of head pitching was controlled by reducer to rotate head joint.

3.2. Motor process analysis of freestyle skiing robot

Competition field of freestyle skiing aerials was made up of start area, speed-up skiing slope, transition area 1, ski jump, transition area 2, landing slope and terminal area [6]. Movement of speed-up skiing phase of freestyle skiing was studied. It can be known after the study on material of freestyle skier in speed-up skiing phase that skiers' postures can be divided into start sliding skiing, squat skiing, standing skiing and body extension preparation. In Changchun University of Technology, H-dimensional laser scanning technique was used to acquire data of skiers in national freestyle skiing aerial team and data of several specific skills were collected. Rotation angles of those four movements of joints are shown in Table 1. Ski-shank angle was included angle of ski and shank. Knee joint angle was included angle of shank and thigh. Hip joint angle was included angle of thigh and trunk in the same side. Shoulder joint angle was included angle of trunk and the upper arm in the same side. Elbow joint angle was included angle of the upper arm and forearm in the same side. Trunk dip angle was included angle of trunk and the snow surface. Neck dip angle was included angle of neck and the snow surface. Head dip angle was included angle of head and the snow surface. Thigh dip angle was included angle of thigh and the snow surface. Ski dip angle was included angle of ski and the snow surface in speed-up skiing phase when slope gradient was changed.

3.3. Gait planning of freestyle skiing robot

3.3.1. Motion curve of freestyle skiing robot in speed-up skiing phase. First, quartic polynomial was used to plan motion curve of 0–3 meters. Then, three cubic polynomials were used to plan motion curve of 3–8 meters, 8–24 meters and 24–52 meters, respectively. Then, quartic polynomial was used to plan motion curve of 52–65 meters. Thus, the whole motion curve was matching with 4–3–3–3–4. Standard global time variable of the whole motion was set as t and local time variable of the jth motion phase was indicated as τ_j. The initial time of each motion phase was $\tau_{j\mathrm{i}}$ and terminal local time of each motion phase was $\tau_{j\mathrm{f}}$. Thus, all motion phases were start from local time of $\tau_{j\mathrm{i}} = 0$ and finish up with the given local time $\tau_{j\mathrm{f}}$. The

equations of those five motion phases are

Table 1. Data acquisition of different phases

Joint angles	Angles in the phase of starting and sliding skiing (°)	Angles of the squat skiing phase (°)	Angles of the body extension preparation phase (°)	Angles of raising arm (°)
Ski-shank	82.25	91.08	79.97	84.17
Knee joint	152.34	123.68	178.05	179.41
Hip joint	153.34	99.40	175.92	176.85
Shoulder joint	13.22	18.77	27.14	160.52
Elbow joint	143.60	138.16	170.02	13.34
Trunk dip angle	82.65	66.80	93.75	100.28
Neck dip angle	75.47	65.44	81.50	86.46
Head dip angle	75.90	73.57	76.38	86.09
Thigh dip angle	109.3	147.41	89.66	97.13

$$\begin{cases} z(t)_1 = a_0 + a_1 t + a_2 t^2 + a_3 t^3 + a_4 t^4, \\ z(t)_2 = b_0 + b_1 t + b_2 t^2 + b_3 t^3, \\ z(t)_3 = c_0 + c_1 t + c_2 t^2 + c_3 t^3, \\ z(t)_4 = d_0 + d_1 t + d_2 t^2 + d_3 t^3, \\ z(t)_5 = e_0 + e_1 t + e_2 t^2 + e_3 t^3 + e_4 t^4. \end{cases} \tag{1}$$

Replacing higher-degree polynomial with multistage low order polynomial, the below equations were obtained:

$$\begin{cases} z_1 = a_0, \\ \dot{z}_1 = a_1, \\ \ddot{z}_1 = 2a_2, \end{cases} \tag{2}$$

$$\begin{cases} z_2 = a_0 + a_1\tau_{1\mathrm{f}} + a_2\left(\tau_{1\mathrm{f}}\right)^2 + a_3\left(\tau_{1\mathrm{f}}\right)^3 + a_4\left(\tau_{1\mathrm{f}}\right)^2, \\ z_2 = b_0, \\ a_1 + 2a_2\tau_{1\mathrm{f}} + 3a_3\left(\tau_{1\mathrm{f}}\right)^2 + 4a_4\left(\tau_{1\mathrm{f}}\right)^3 = b_1, \\ 2a_2 + 6a_3\left(\tau_{1\mathrm{f}}\right) + 12a_4\left(\tau_{1\mathrm{f}}\right)^2 = 2b_2, \end{cases} \tag{3}$$

$$\begin{cases} z_3 = b_0 + b_1\tau_{2\mathrm{f}} + b_2\left(\tau_{2\mathrm{f}}\right)^2 + b_3\left(\tau_{2\mathrm{f}}\right)^3, \\ z_3 = c_0, \\ b_1 + 2b_2\tau_{2\mathrm{f}} + 3b_3\left(\tau_{2\mathrm{f}}\right)^2 = c_1, \\ 2b_2 + 6b_3\left(\tau_{2\mathrm{f}}\right) = 2c_2, \end{cases} \tag{4}$$

$$\begin{cases} z_4 = c_0 + c_1\tau_{3\mathrm{f}} + c_2\left(\tau_{3\mathrm{f}}\right)^2 + c_3\left(\tau_{3\mathrm{f}}\right)^3, \\ z_4 = d_0, \\ c_1 + 2c_2\tau_{3\mathrm{f}} + 3c_3\left(\tau_{3\mathrm{f}}\right)^2 = d_1, \\ 2c_2 + 6c_3\left(\tau_{3\mathrm{f}}\right) = 2d_2, \end{cases} \tag{5}$$

$$\begin{cases} z_5 = d_0 + d_1\tau_{4\mathrm{f}} + d_2\left(\tau_{4\mathrm{f}}\right)^2 + d_3\left(\tau_{4\mathrm{f}}\right)^3, \\ z_5 = e_0, \\ d_1 + 2d_2\tau_{4\mathrm{f}} + 3d_3\left(\tau_{4\mathrm{f}}\right)^2 = e_1, \\ 2d_2 + 6d_3\left(\tau_{4\mathrm{f}}\right) = 2e_2, \end{cases} \tag{6}$$

$$\begin{cases} z_6 = \mathrm{e}_0 + e_1\tau_{5\mathrm{f}} + e_2\left(\tau_{5\mathrm{f}}\right)^2 + e_3\left(\tau_{5\mathrm{f}}\right)^3 + e_4\left(\tau_{5\mathrm{f}}\right)^2, \\ \dot{z}_6 = \mathrm{e}_1 + 2e_2\left(\tau_{5\mathrm{f}}\right) + 3e_3\left(\tau_{5\mathrm{f}}\right)^2 + 4e_4\left(\tau_{5\mathrm{f}}\right)^3, \\ \ddot{z}_6 = 2e_2 + 6e_3\left(\tau_{5\mathrm{f}}\right) + 12e_4\left(\tau_{5\mathrm{f}}\right)^2. \end{cases} \tag{7}$$

Substituting those known data –$z_1 = 0$, $\dot{z}_1 = 1$, $\ddot{z}_1 = 0$, $\tau_{1f} = 1$, $z_2 = 3$, $\tau_{2f} = 1$, $z_3 = 8$, $\tau_{3f} = 2$, $z_4 = 24$, $\tau_{4f} = 2$, $z_5 = 52$, $\tau_{5f} = 1$, $\dot{z}_6 = 16$ and $\ddot{z}_6 = 2$ to above equations, motion equation of freestyle skiing robot in speed-up skiing phase can obtained and shown in equation (8).

$$\begin{cases} z_1 = t + 0.5t^2 + 3.17t^3 - 1.67t^4, \\ z_2 = 3 + 4.83t - 0.0036t^2 + 0.17t^3, \\ z_3 = 8 + 5.34t + 0.51t^2 + 0.41t^3, \\ z_4 = 24 + 12.3t + 3t^2 - 1.06t^3, \\ z_5 = 52 + 11.46t - 3.39t^2 + 8.39t^3 - 3.46t^4, \end{cases} \tag{8}$$

3.3.2. Motion curve planning of hip joint. Given motion curve equation of hip joint. In the second motion phase it can be written as

$$\theta_{\mathrm{h}2}(t) = f_{20} + f_{21}t + f_{22}t^2 + f_{23}t^3 + f_{24}t^4 + f_{25}t^5. \tag{9}$$

Substitute boundary conditions to equation (9), the below equation can be obtained:

$$\begin{cases} 153 = f_{20}, \\ 100 = f_{20} + f_{21} + f_{22} + f_{23} + f_{24} + f_{25}, \\ 0 = f_{21}, \\ 0 = f_{21} + 2f_{22} + 3f_{23} + 4f_{24} + 5f_{25}, \\ 0 = 2f_{22}, \\ 0 = 2f_{22} + 6f_{23} + 12f_{24} + 20f_{25}, \end{cases} \tag{10}$$

Thus, the polynomial equation of location is obtained in the form

$$\theta_{\mathrm{h}2}(t) = 153 - 530t^3 + 795t^4 - 318t^5. \tag{11}$$

The motion curve equation of hip joint in the fourth motion phase is

$$\theta_{\mathrm{h}4}(t) = f_{40} + f_{41}t + f_{42}t^2 + f_{43}t^3 + f_{44}t^4 + f_{45}t^5. \tag{12}$$

Substituting boundary conditions to equation (12), the below equation is obtained:

$$\begin{cases} 100 = f_{40}, \\ 176 = f_{40} + 2f_{41} + 4f_{42} + 8f_{43} + 16f_{44} + 32f_{45}, \\ 0 = f_{41}, \\ 0 = f_{41} + 4f_{42} + 12f_{43} + 32f_{44} + 80f_{45}, \\ 0 = 2f_{42}, \\ 0 = 2f_{42} + 12f_{43} + 48f_{44} + 160f_{45}. \end{cases} \tag{13}$$

Thus, polynomial equation of location was:

$$\theta_{\mathrm{h4}}(t) = 100 + 95t^3 - 71.25t^4 + 14.25t^5 . \tag{14}$$

Equations of five motion phases of hip joint were obtained as follows

$$\begin{cases} \theta_{\mathrm{h1}}(t) = 153, & 0 < t \le 1, \\ \theta_{\mathrm{h2}}(t) = 153 - 530t^3 + 795t^4 - 318t^5, & 0 < t \le 1, \\ \theta_{\mathrm{h3}}(t) = 100, & 0 < t \le 2, \\ \theta_{\mathrm{h4}}(t) = 100 + 95t^3 - 71.25t^4 + 14.25t^5, & 0 < t \le 2, \\ \theta_{\mathrm{h5}}(t) = 176, & 0, < t \le 1. \end{cases} \tag{15}$$

3.3.3. Motion curve planning of knee joint. Given motion curve of knee joint. In the second motion phase it has the form

$$\theta_{k2}(t) = g_{20} + g_{21}t + g_{22}t^2 + g_{23}t^3 + g_{24}t^4 + g_{25}t^5 . \tag{16}$$

Substitute boundary conditions in (16), the below equation can be obtained

$$\begin{cases} 153 = g_{20}, \\ 124 = g_{20} + g_{21} + g_{22} + g_{23} + g_{24} + g_{25}, \\ 0 = g_{21}, \\ 0 = g_{21} + 2g_{22} + 3g_{23} + 4g_{24} + 5g_{25}, \\ 0 = 2g_{22}, \\ 0 = 2g_{22} + 6g_{23} + 12g_{24} + 20g_{25}. \end{cases} \tag{17}$$

Thus, polynomial equation of location has the form

$$\theta_{\mathrm{k2}}(t) = 153 - 290t^3 + 435t^4 - 174t^5 . \tag{18}$$

Given motion curve equation of knee joint in the fourth motion phase as

$$\theta_{\mathrm{k4}}(t) = g_{40} + g_{41}t + g_{42}t^2 + g_{43}t^3 + g_{44}t^4 + g_{45}t^5 . \tag{19}$$

Substituting boundary conditions to equation (19) provides

$$\begin{cases} 100 = g_{40}, \\ 176 = g_{40} + 2g_{41} + 4g_{42} + 8g_{43} + 16g_{44} + 32g_{45}, \\ 0 = g_{41}, \\ 0 = g_{41} + 4g_{42} + 12g_{43} + 32g_{44} + 80g_{45}, \\ 0 = 2g_{42}, \\ 0 = 2g_{42} + 12g_{43} + 48g_{44} + 160g_{45}. \end{cases} \tag{20}$$

Thus, the polynomial equation of location can be obtained in the form

$$\theta_{\mathrm{k4}}(t) = 124 + 67.5t^3 - 50.63t^4 + 10.13t^5 \tag{21}$$

Thus, equations of five motion phases of knee joint reads

$$\begin{cases} \theta_{\mathrm{k1}}(t) = 153, & 0 < t \le 1, \\ \theta_{\mathrm{k2}}(t) = 153 - 290t^3 + 435t^4 - 174t^5, & 0 < t \le 1, \\ \theta_{\mathrm{k3}}(t) = 124, & 0 < t \le 2, \\ \theta_{\mathrm{k4}}(t) = 124 + 67.5t^3 - 50.63t^4 + 10.13t^5, & 0 < t \le 2, \\ \theta_{\mathrm{k5}}(t) = 178, & 0 < t \le 1. \end{cases} \tag{22}$$

3.3.4. Motion curve planning of shoulder joint. The motion curve equation of shoulder joint in the second motion phase is

$$\theta_{\mathrm{s2}}(t) = h_{20} + h_{21}t + h_{22}t^2 + h_{23}t^3 + h_{24}t^4 + h_{25}t^5 . \tag{23}$$

After substituting the boundary conditions into equation (23) we get

$$\begin{cases} 10 = h_{20}, \\ 80 = h_{20} + h_{21} + h_{22} + h_{23} + h_{24} + h_{25}, \\ 0 = h_{21}, \\ 0 = h_{21} + 2h_{22} + 3h_{23} + 4h_{24} + 5h_{25}, \\ 0 = 2h_{22}, \\ 0 = 2h_{22} + 6h_{23} + 12h_{24} + 20h_{25}. \end{cases} \tag{24}$$

Thus, the polynomial equation of location is

$$\theta_{\mathrm{s2}}(t) = 10 + 700t^3 - 1050t^4 + 420t^5 . \tag{25}$$

The motion curve equation of shoulder joint in the fourth motion phase is

$$\theta_{\mathrm{s4}}(t) = h_{40} + h_{41}t + h_{42}t^2 + h_{43}t^3 + h_{44}t^4 + h_{45}t^5 . \tag{26}$$

After substituting the boundary conditions to equation (26), we obtain

$$\begin{cases} 120 = h_{40}, \\ 10 = h_{40} + 2h_{41} + 4h_{42} + 8h_{43} + 16h_{44} + 32h_{45}, \\ 0 = h_{41}, \\ 0 = h_{41} + 4h_{42} + 12h_{43} + 32h_{44} + 80h_{45}, \\ 0 = 2h_{42}, \\ 0 = 2h_{42} + 12h_{43} + 48h_{44} + 160h_{45}\,. \end{cases} \tag{27}$$

Thus, the polynomial equation of location has the following form

$$\theta_{\mathrm{s}4}(t) = 120 - 137.5t^3 + 103.13t^4 - 20.63t^5\,. \tag{28}$$

Thus, equations of five motion phases of shoulder joint are

$$\begin{cases} \theta_{\mathrm{s}1}(t) = 10, & 0 < t \le 1, \\ \theta_{\mathrm{s}2}(t) = 10 + 700t^3 - 1050t^4 + 420t^5, & 0 < t \le 1, \\ \theta_{\mathrm{s}3}(t) = 120, & 0 < t \le 2, \\ \theta_{\mathrm{s}4}(t) = 120 - 137.5t^3 + 103.13t^4 - 20.63t^5, & 0 < t \le 2, \\ \theta_{\mathrm{s}5}(t) = 10, & 0 < t \le 1. \end{cases} \tag{29}$$

3.3.5. Motion curve planning of elbow joint The motion curve equation of elbow joint in the second motion phase is

$$\theta_{e2}(t) = k_{20} + k_{21}t + k_{22}t^2 + k_{23}t^3 + k_{24}t^4 + k_{25}t^5\,. \tag{30}$$

After substituting the boundary conditions to equation (30)we obtain

$$\begin{cases} 144 = k_{20}, \\ 138 = k_{20} + k_{21} + k_{22} + k_{23} + k_{24} + k_{25}, \\ 0 = k_{21} \\ 0 = k_{21} + 2k_{22} + 3k_{23} + 4k_{24} + 5k_{25}, \\ 0 = 2k_{22}, \\ 0 = 2k_{22} + 6k_{23} + 12k_{24} + 20k_{25}, \end{cases} \tag{31}$$

The polynomial equation of location has the form

$$\theta_{\mathrm{e}2}(t) = 144 - 60t^3 + 90t^4 - 36t^5\,. \tag{32}$$

The motion curve location of elbow joint in the fourth motion phase is

$$\theta_{\mathrm{e}4}(t) = k_{40} + k_{41}t + k_{42}t^2 + k_{43}t^3 + k_{44}t^4 + k_{45}t^5\,. \tag{33}$$

After substituting the boundary conditions to equation (33), we obtain

$$\begin{cases} 138 = k_{40}, \\ 170 = k_{40} + 2k_{41} + 4k_{42} + 8k_{43} + 16k_{44} + 32k_{45}, \\ 0 = k_{41}, \\ 0 = k_{41} + 4k_{42} + 12k_{43} + 32k_{44} + 80k_{45}, \\ 0 = 2k_{42}, \\ 0 = 2k_{42} + 12k_{43} + 48k_{44} + 160k_{45}. \end{cases} \tag{34}$$

Now, the polynomial equation of location has the form

$$\theta_{c4}(t) = 138 + 40t^3 - 30t^4 + 6t^5 . \tag{35}$$

Finally, the equations of five motion phases of elbow joint may be written as

$$\begin{cases} \theta_{e1}(t) = 144, & 0 < t \le 1, \\ \theta_{e2}(t) = 144 - 60t^3 + 90t^4 - 36t^5, & 0 < t \le 1, \\ \theta_{e3}(t) = 138, & 0 < t \le 2, \\ \theta_{e4}(t) = 138 + 40t^3 - 30t^4 + 6t^5, & 0 < t \le 2, \\ \theta_{e5}(t) = 170, & 0 < t \le 1. \end{cases} \tag{36}$$

4. Motion simulation of freestyle skiing robot

4.1. Virtual prototype modeling of freestyle skiing robot

The simplified model of freestyle skiing robot built in Pro/E was saved as file type "Parasolid". Import it into software ADAMS then its rigid body component attribute was modified and constraint and motion drive was added. Motion curve of all joints of freestyle skiing robot was used as control basis, which was input in ADAMS to generate STEP function. Simulation analysis of motion of freestyle skiing robot was conducted.

4.2. Motion simulation and its results analysis of freestyle skiing robot

Motion curves of all joints of freestyle skiing robot obtained through gait planning was used as control basis and those motion curves was parameterized to generate STEP functions. Driving function of all joints obtained through gaiting planning is shown in Table 2. Then, the STEP functions were added to the corresponding joints of freestyle skiing robot of virtual prototype. Before simulation analysis, check prototype model again. Interactive kinematics simulation of freestyle skiing robot was conducted.

Table 2. STEP driving function of all joints

Joints name	STEP FUNCTION
Ankle joint	0d×time
Knee joint	STEP(time,1,0d,2,29d) + STEP(time,4,0d,6,-54d)
Hip joint	STEP(time,1,0d,2,-53d) + STEP(time,4,0d,6,76d)
Shoulder joint (Roll)	STEP(time,6,0d,7,-180d)
Shoulder joint (Pitching)	STEP(time,1,0d,2,70d) + STEP(time,4,0d,6,-70d)
Waist joint	0d×time
Sliding movement	STEP(time,0,0,1,3000) + STEP(time,1,0,2,5000) + STEP(time,2,0,4,16000) + STEP(time,4,0,6,28000) + STEP(time,6,0,7,13000)

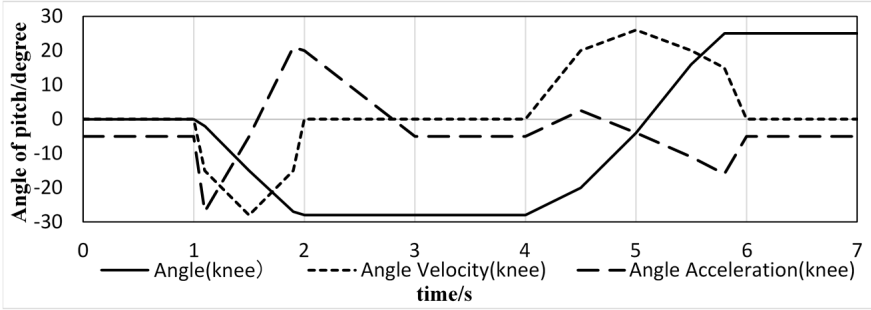

Fig. 1. Pitching of right knee joint

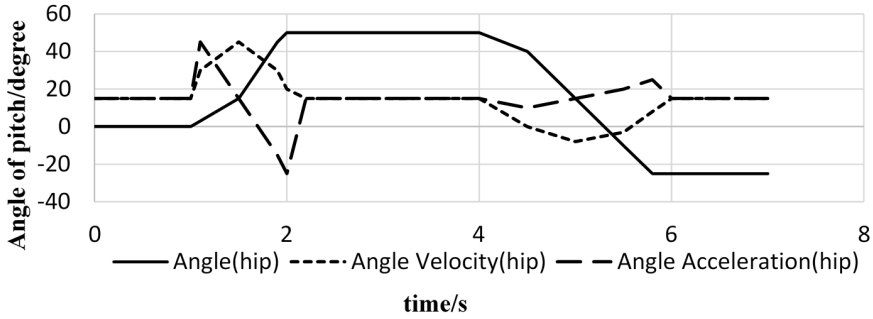

Fig. 2. Pitching of right hip joint

Experimental simulations show that freestyle skiing robot can dynamically simulate speed-up skiing phase well, including starting and sliding skiing, squat skiing, body extension preparation and raising arm. Then, post-processing module ADAMS/Post-Processor was used for post-process simulation analysis of results of

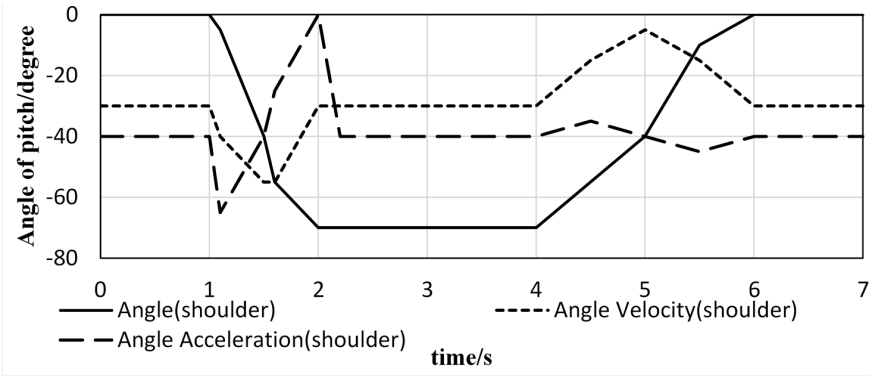

Fig. 3. Pitching of right shoulder joint

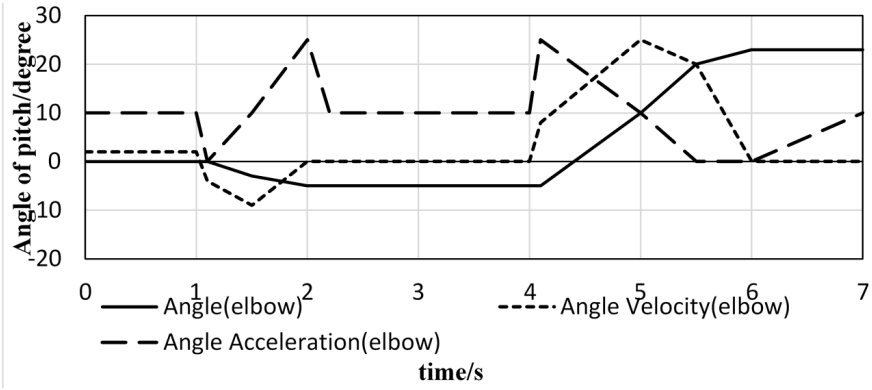

Fig. 4. Pitching of right elbow joint

ADAMS software. With this function, results of simulation calculation and analysis research of ADAMS can be displayed, thus model characteristics was reflected more accurately. Simulation curves of angular displacement, speed, and accelerated speed of joints rotation of freestyle skiing robot during movement are shown in Figs. 1–4. Because freestyle skiing robot was a symmetrical structure, simulation curve of the right arm joint and right leg joint was chosen.

5. Conclusion

Pro/E with powerful modeling function is used to build the simplified mechanical model of freestyle skiing robot. Virtual prototype of freestyle skiing robot is built in ADAMS for motion simulation. The simulation results show that bionic gait planning is suitable for motion planning of freestyle skiing robot, with which all movements of freestyle skiing robot in speed-up skiing phase are achieved.

References

[1] Z. Liu, C. Chen, Y. Zhang: *Decentralized robust fuzzy adaptive control of humanoid robot manipulation with unknown actuator backlash.* IEEE Transactions on Fuzzy Systems *23* (2015), No. 3, 605–616.

[2] H. Gritli, S. Belghith, N. Khraief: *OGY-based control of chaos in semi-passive dynamic walking of a torso-driven biped robot.* Nonlinear Dynamics *79* (2015), No. 2, 1363–1384.

[3] L. Žlajpah: *Simulation in robotics.* Mathematics and Computers in Simulation *79* (2008), No. 4, 879–897.

[4] Q. Nguyen, K. Sreenath: *L1 adaptive control for bipedal robots with control Lyapunov function based quadratic programs.* Proc. IEEE American Control Conference (ACC), 1–3 July 2015, Chicago, IL, USA, IEEE Conference Publications (2015), 862–867.

[5] D. Rollinson, A. Buchan, H. Choset: *Virtual chassis for snake robots: Definition and applications.* Advanced Robotics *26* (2012), No. 17, 2043–2064.

[6] X. Wang, Y. Ma, Q. W. Hao: *Kinematic analysis on Chinese female athletes' bFdF action in freestyle skiing aerialse.* International Journal of Advancements in Computing Technology *4* (2012), No. 16, 175–182.

Received May 7, 2017